Biomolecules and Biomedicine
ISSN: 2831-0896 (Print) | ISSN: 2831-090X (Online)
Journal Impact Factor® (2024): 2.2
CiteScore® (2024): 5.2
www.biomolbiomed.com | blog.bjbms.org

RESEARCH ARTICLE

Deniz et al: Melatonin and Omega-3 in EMF Exposure

Melatonin and omega-3 neuroprotection in prenatal rat spinal cord exposed to 900 MHz electromagnetic field

Ömür Gülsüm Deniz[1*], Gamze Altun[2], Süleyman Kaplan[2]

[1]Department of Histology and Embryology, Faculty of Medicine, Bolu Abant İzzet Baysal University, Bolu, Türkiye

[2]Department of Histology and Embryology, Ondokuz Mayıs University, Samsun, Türkiye

[*]Correspondence to Ömür Gülsüm Deniz: omur.denizomu@gmail.com

DOI: https://doi.org/10.17305/bb.2025.12633

ABSTRACT

The electromagnetic field (EMF) emitted by electronic devices induces pathological changes in tissues, adversely affecting embryonic and pubertal development. This study investigates the effects of melatonin (Mel) and omega-3 fatty acids (ω3) on the spinal cord in rats exposed to EMF, employing stereological methods alongside light and electron microscopic evaluations. Pregnant Wistar albino rats were divided into seven groups: Control (CONT), sham-exposed (SHAM), EMF alone, EMF-Mel, EMF-ω3, Mel only, and ω3 only. The EMF, EMF-Mel, and EMF-ω3 groups were exposed to a 900 MHz EMF for two hours daily during the prenatal period (21 days). Mel and ω3 were administered via intragastric gavage prior to EMF exposure. Upon completion of the experiment (on the 35th day post-birth), spinal cord tissues of all male offspring were dissected and subjected to light and ultrastructural examinations. Stereological analyses calculated grey matter (GM) to total volume ratios, white matter (WM) to total volume ratios, GM to WM volume ratios, total spinal cord volume, and motor neuron counts. No significant differences were observed among the groups regarding GM/WM volume ratios, GM/total volume ratios, WM/total volume ratios, and total spinal cord volume ($p > 0.05$). However, a significant reduction in motor neuron numbers was noted in the EMF-ω3 group compared to the CONT group ($p < 0.01$). Light and ultrastructural examinations revealed marked motor neuron degeneration and axonal disruption in the EMF group, which were mitigated in the Mel and ω3-treated groups. These findings indicate that prenatal exposure to 900 MHz EMF exerts detrimental effects on spinal cord tissue and underscore the necessity for further studies exploring varying doses and durations to elucidate the potential effects of ω3 and Mel.

Keywords: Electromagnetic field, neuroprotection, physical disector, Cavalieri principle, ultrastructure, spinal cord.

INTRODUCTION

The rapid development of technology is significant in terms of both the benefits it provides and also of the individual and social side-effects it may cause. The number of technological devices that become part of daily life increases rapidly as a result of these developments. The number of technological devices that cause electromagnetic field (EMF) effects is also high. Studies show that exposure to ever-increasing EMF effects will lead to pathological outcomes. It is therefore important to investigate the effects of EMF exposure on human health [1]. The most important source of EMF with an individual impact on human health is mobile phones, which have now become indispensable items, and the transmitters that enable communication with such phones. This is because mobile phones are the EMF sources used in the closest proximity to the human body. The EMF emitted by mobile phones produces very significant effects on living tissue. These effects manifest themselves in different ways in diverse tissues and organs [2]. Numerous studies have reported that specific levels of EMF cause morphological, biochemical, and physiological changes in organs such as the testis, brain, ovary, liver, kidney and spinal cord, which may lead to reversible or irreversible pathologies [3-8]. Depending on the amount and duration of exposure, EMF has been reported to result in particularly deleterious effects in the central nervous system [6, 9, 10].

Antioxidants exhibit protective effects against the oxidative damage caused by free oxygen radicals. A state of balance exists between free oxygen radicals and antioxidants. Preserving this balance is essential for the organism to maintain its vital functions. Melatonin (Mel) is one of the most powerful antioxidants used today. Thanks to its hydrophilic properties, it easily crosses the blood-brain barrier, and it can diffuse rapidly to all subcellular compartments [11, 12]. In addition to its antioxidant activity, it also exhibits numerous anti-inflammatories, anticarcinogenic, neuroprotective and anti-aging bioactivities. Beyond that, Mel, a neuroprotective agent with receptors in the fetal brain [13], can show a dose-dependent effect against brain damage [14]. In this context, this agent has a critical role in fetal development [15].

Omega-3 (ω3) is an unsaturated fatty acid with antioxidant properties. It cannot be manufactured by the body and must be absorbed from the outside through diet [16]. ω-3 fatty acids, which participate in the structure of the cell membrane, are necessary for the cells to maintain their normal functions. They also possess antioxidant, anti-inflammatory, antihypertensive, antihyperlipidemic and antiatherogenic properties. They are particularly abundant in the brain, spinal cord, retina, and other neural tissues, and play an important role

in the development of the nervous system. They contribute to the healthy transmission of electrical impulses by protecting the axonal structure [17].

Pathological changes that may occur because of damage to spinal cord tissue may cause problems in signal transmission between the brain and the peripheral nervous system [9]. Our examination of the current literature revealed few studies investigating the effects of 900 MHz EMF on the spinal cord. This study was therefore to investigate the effects of Mel and ω3 on the spinal cords of male pups exposed to 900 MHz EMF in the prenatal period using stereological methods, one of the unbiased and reliable histomorphometric methods, light and electron microscopic evaluations, and thus to contribute to the existing literature.

MATERIALS AND METHODS

Animals and group design

Spinal cords of the animals were used in the present study (Ondokuz Mayıs University animal experiments local ethics committee, 68489742-604.01.03-E.5621 and date: 07.03.2019). The spinal cords, which were dissected during the experiment after perfusion, were tissue of the study (2018/24 and 05.04.2018). The well-being of the experimental animals and ethical principles were taken into consideration during the entire experiment. All experimental procedures were carried out accordance with the U.K. Animals (Scientific Procedures) Act, 1986 and associated guidelines, EU Directive 2010/63/EU for animal experiments, or the National Institutes of Health guide for the care and use of Laboratory animals (NIH Publications No. 8023, revised 1978).” in the related section.

Thirty-five adults female *Wistar albino* rats were initially randomly divided into seven groups of five animals each. These were left to mate with male rats in separate cages. Rats with sperm detected in vaginal smear samples were regarded being on day 0 of pregnancy. These pregnant rats were housed in separate cages at room temperature and 40-50% humidity in a 12-hour light/dark cycle. Ad libitum access to water and standard chow was permitted throughout the experiment.

A power analysis test was conducted using Minitab version 18.0 to determine the requisite number of animals in all groups. In this context, pregnant rats were divided into seven groups, Control (CONT), SHAM, 900 MHz EMF exposure (EMF), a group receiving Mel before 900 MHz EMF exposure (EMF-Mel), a group receiving ω3 prior to 900 MHz EMF exposure (EMF-ω3), a group receiving Mel only (Mel) and one receiving ω3 only (ω3). Female rats in the SHAM group were placed in the EMF exposure system during the gestational period (21

days) but were not treated with EMF. Pregnant rats in the EMF, EMF-Mel, and EMF-ω3 groups were exposed to 900 MHz EMF throughout the gestational period. As in the groups given only Mel and ω3, EMF-Mel and EMF-ω3 groups received 50 mg/kg/day Mel (Lyophilized Melatonin Powder M5250 10 g, Sigma-Aldrich, Germany) and 1ml/kg/day ω3 (F8020, Sigma-Aldrich, Germany), respectively, via intragastric gavage before EMF exposure.Ready form solution of ω3 (Sigma Aldrich, Germany) at a concentration of 0.93 g/ml was used. The female rats that had mated before the experiment were randomly divided into groups. Since there were five pregnant rats in each group, at least 10 male newborn rats were obtained from each group at the end of the pregnancy period. They stayed with the mother rats after birth. Male offspring born to mothers belonging to each group (n=5) were randomly selected.Postnatally, male offspring rats (n=10) were housed in separate cages after weaning and were sacrificed 35 days after birth.

EMF exposure system

Pregnant rats from the EMF exposure groups were housed in an EMF exposure system with a 0-9 W output signal generator (Microwave Test Transmitter, Set Electronic Ltd, Turkey) emitting 900 MHz radiofrequency (RF)-EMF waves for 2 hours a day for 21 days. RF waves were emitted using a monopole antenna. The rats' head region was located 3.6 cm from the antenna. During exposure, the rats were kept in an experimental Plexiglas setup of 16 equal chambers. Holes in the top allowed the rats to breathe. The electric field value was measured with an RF-EMF strength meter (Extech Instruments Corporation, USA). Measurements from the caudal region taken every six minutes during the experiment were recorded in V/m. EMF exposure during experiments was performed in an isolated room that reduced unwanted exposure from the outside.

Paraffin blocks of spinal cord tissue

Thirty-five days after birth, 70 male offspring rats were exposed to intracardiac perfusion under anaesthesia using a mixture of ketamineand xylazine, respectively (50 mg/kg-10 mg/kg, intraperitoneally). For perfusion, 0.9% physiological serum was administered intracardially to ensure that the blood was completely cleared from the vessels. Following this procedure,10% formalin solution was administered intracardially for three to four minutes. After perfusion, spinal cord tissues were dissected at the C3-C5 level. Tissue samples were fixed in a 10% formaldehyde solution to obtain paraffin blocks and in 4% glutaraldehyde to produce resin blocks. Tissues with complete fixation were included in the routine tissue follow-up procedure and embedded in paraffin blocks. Sections were taken from paraffin blocks according to the

systematic sample rule, which is an unbiased and efficient method for selecting sample sites within the region of interest. They were then stained with cresyl violet (C5042-10 g, Sigma-Aldrich, Germany) and subjected to histopathological evaluations and stereological analyses.In this context, related images were obtained using a light microscope compatible with the computer-aided cellSens Entry software (Olympus, Center Valley, PA, USA). During paraffin embedding processes, all sampled were coded for the sake of all analyses would be done blindly.

Sectioning and stereological analysis

Following the pilot study, sections of 4 µm in thickness were taken from paraffin-embedded spinal cord tissues at a ratio of 1/15 (every 15^{th} section and its adjacent section for disector pair)in the coronal plane according to the systematic random sampling rule for stereological analyses. After deparaffinization, the physical disector method was used estimate the numbers of motor neurons in the cresyl violet stained sections **(Figures 1C and 1D).**The counting unit in the present study was the neuronal nucleus. Additionally, the area of the unbiased counting frame used was 5,925 μm^2. The total volume of spinal cord samples was calculated using the Cavalieri method [18] **(Figures 1A and 1B).** In addition, ratios of grey matter (GM)/total volume, white matter (WM)/total volume, and GM/WM volume were estimated using a point counting grid (one point area: 2500 μm^2). The appropriate coefficient of error (CE≤0.05) for each subject and the appropriate coefficient of variation (CV≤0.20) for each group were considered during stereological estimations [18, 19].

Preparation of resin blocks for light and electron microscopy

Following perfusion, the spinal cord tissues fixed in 4% glutaraldehyde solution were dissected in a 1 mm^3 volume under a stereomicroscope, and an electron microscopic tissue tracking procedure was applied[19].In this context, tissues were treated with phosphate buffer (0.1 M PBS) before processing. Post-fixation was completed by treating the tissues with 1% osmium tetroxide (Sigma, St. Louis, MO). Tissues were then dehydrated by being passed through graded acetones (50%, 70%, 96%, and 100%) and were transferred to propylene oxide (Sigma-Aldrich Co.). After, they were placed into an araldite (CY212, Agar Scientific Ltd, Essex, UK)-propylene oxide mixturefollowed by pure araldite. The spinal cord tissues were embedded in resin Molds at 45 °C. The resin Molds were dried overnight, subsequently placed in an oven at 50 °C, adjusted every 30 minutes. In this regard, the polymerization process of the tissues, involving a temperature increase every half hour (45-50° C-55°C), was

completed at 62° C for 48 hours. The tissue resin blocks were then ready for sectioning using an ultramicrotome.

Toluidine blue staining and transmission electron microscopy

Semi-thin sections (500 nm) for light microscopic evaluation and thin sections (70 nm) for electron microscopic evaluation were taken from the resin-embedded tissues. Semi-thin sections were stained with 1% toluidine blue (Sigma-Aldrich Co. LLC., St. Louis, USA) prepared as a combination of 1% toluidine blue, 2% sodium borate, and 10 ml distilled water. Thin sections were placed on copper grids and stained in the automatic contrast system (Leica EM AC20, Leica Microsystems GmbH, Germany) using 0.5 % uranyl acetate and 3 % lead citrate. Electron microscopy (JEOL JSM-7001F, JEOL Ltd., Tokyo, Japan) was used for ultrastructure-level images taken from the sections.Electron microscopic examinations were performed at the Imaging and Characterization Unit of the Ondokuz Mayıs University Karadeniz Advanced Technical Research and Application Center.

Ethical statement

This study was approved by the Ondokuz Mayıs University animal experiments local ethics committee under 68489742-604.01.03-E.5621 and date: 07.03.2019. All experimental procedures were carried out accordance with the U.K. Animals (Scientific Procedures) Act, 1986 and associated guidelines, EU Directive 2010/63/EU for animal experiments, or the National Institutes of Health guide for the care and use of Laboratory animals (NIH Publications No. 8023, revised 1978).

Statistical analysis

Statistical analyses were conducted using SPSS version 21.0 software. The Shapiro-Wilk test was used to evaluate whether the data conformed with the assumption of normal distribution. In the comparison of continuous variables, normally distributed data were evaluated with One-Way ANOVA and the Bonferroni test as post-hoc. Kruskal-Wallis analysis and the Bonferroni corrected Mann-Whitney U test as post-hoc were used in the comparison non-normally distributed multiple groups. $p<0.05$ were considered statistically significant.

RESULTS

Histopathological analysis

Light microscopic evaluation of cresyl violet stained sections

Cresyl violet stained sections from all groups were examined histopathologically at the light microscopic level. In this context, histopathological examination of the study tissue sectionsrevealed a normal general structure in the spinal cord and motor neurons in the CONT **(Figure2b)**, SHAM **(Figure2c)**, Mel **(Figure 2d)**, and ω3 **(Figure2e)** group sections. Light microscopic examination showed that the boundaries of the perikarya of motor neurons were clear and distinct. Sugimoto et al. [20] reported that damaged neurons possessed three main features, irregular cellular outlines and increased chromatin density in the nucleus and cytoplasm **(Figure 2f).** Large numbers of nuclei that had lost euchromatic properties and motor neurons with narrow and dark stained cytoplasm were observed in the EMF group **(Figure2f)**. Cell boundaries were indistinct in most of the motor neurons from this group. In particular, the borders of degenerating neurons were indistinguishable. In some areas, the cell borders of these damaged neurons were undetectable. In addition, healthy-appearing motor neurons in the EMF-Mel **(Figure 2g)** and EMF-ω3 **(Figure 2h)** groups were than in the EMF group. Furthermore, degeneration in the EMF-ω3 group was greater than in the EMF-Mel group.

Light microscopic evaluation of toluidine blue stained semi-thin sections

The morphologies of neurons, neuroglia cells, and axons were examined and evaluated histopathologically in semi-thin sections from all groups using light microscopy. In this context, when semi-thin sections obtained from sections stained with toluidine blue were examined, it was observed that the motor neurons and neuroglia cells of the CONT **(Figure 3a)**, SHAM**(Figure3c)**, Mel **(Figure3e)** and ω3 groups**(Figure3g)** had normal morphology. It was determined that the motor neurons located in the gray matter were oval-shaped, had regular borders, euchromatic nuclei, and there were neuroglia cells between them. In addition, it was observed that the intercellular space was normal and the integrity with the surrounding tissue was preserved. Apart from this, when the axonal structure was examined in the relevant groups; the axons in the CONT **(Figure 3b)** and ω3 **(Figure 3h)** groups exhibited a healthy morphology, while the integrity of the connective tissue adjacent to the axon was well preserved. Although axonal degeneration was seen in some places in the SHAM group **(Figure 3d)**, it was observed that the healthy axons were denser. In addition, myelinated

axons of both healthy and degraded morphology were observed in the Mel-only group **(Figure 3f)**.

When semi-thin sections from the EMF **(Figure 4a)**, EMF-Mel **(Figure 4c)** and EMF-ω3 **(Figure 4e)** groups were evaluated histopathologically in terms of motor neuron morphology, vacuolization around the motor neurons was noted. In addition, serious axonal degradation and oligodendrocyte degeneration were detected in the EMF group **(Figure 4b)**. In the EMF-Mel **(Figure 4d)** and EMF-ω3 **(Figure 4f)** groups, it was observed that the deleterious effects of EMF on the structures were alleviated and healthy axons and oligodendrocytes that preserved their morphology were abundant.

Electron microscopic evaluation

The ultrastructure of the motor neurons in the CONT group appeared healthy, with distinct boundaries of the nucleus and nucleolus readily observable. The borders of the glial cell nuclei were clearly defined, and their nuclear structures were oval and stained with euchromatin **(Figure 5a)**. The SHAM group demonstrated a robust structure, with nuclei exhibiting euchromatic staining. The boundaries of the nucleus and nucleolus were clearly delineated **(Figure 5b)**. The ultrastructure of neurons in the EMF group revealed indistinct nuclear cell borders. In this situation, the boundaries of neurons were distorted, having relinquished their spherical form. Additionally, several vacuolization was noted surrounding motor neurons **(Figure5c)**. Furthermore, the EMF-Mel **(Figure 5d)** and EMF-ω3 **(Figure 5e)** groups demonstrated that the neurons displayed a normal morphology. The integrity of the nuclear membrane was notably preserved in these groups. Furthermore, the overall morphology of the neurons in the Mel **(Figure5f)** and ω3 groups **(Figure 5g)** appeared to be intact. The oligodendroglia in the ω3 group displayed a normal structure, characterized by distinctly conspicuous nuclei and nucleoli.

Stereological evaluation

In the relevant study, volume analyses were performed using the Cavalieri principle and motor neuron counting was calculated using the physical disector counting method, which are unbiased and reliable stereological methods. In this context, no significant difference was found among the groups regarding total volume ($p>0.05$). Similarly, the volume fractions of GM/WM, GM/total volume, and WM/total volume showed no significant differences between the groups ($p>0.05$) **(Figures 6-9).** However, when the groups were evaluated in terms of motor neuron number, a significant difference was found among the groups ($p<0.01$) **(Figure 10).** From that perspective, a significant decrease in the number of motor neurons was

observed in the EMF-ω3 group compared to the CONT group (p<0.01). Besides, the EMF-ω3 group exhibited a significantly lower number of motor neurons than the MEL group (p<0.05).

DISCUSSION

High doses of and prolonged exposure to EMF during pregnancy are known to trigger cell death and inhibit neural stem cell differentiation in the prenatal and postnatal periods [21]. Deleterious effects resulting from various teratogenic factors in the embryonal and foetal period occur more in the prenatal period than in the postnatal period [22]. The embryo is highly sensitive to toxic agents in the first two weeks of the embryonic period. The teratogenic effects of EMF exposure in the prenatal period have therefore attracted the attention of researchers due to the current widespread use of mobile phones. Considering the sensitivity of the foetus to maternal effects, it is important to investigate the effects of EMF exposure in the prenatal period on the central nervous system in detail. The adverse effects of EMF exposure on the central nervous system have started to be examined, particularly due to mobile phones being used in close proximity to the head [6, 10, 23].Yahyazadeh and Altunkaynak[24] showed that exposure to a 900 MHz EMF caused adverse effects in the rat spinal cord. Another study conducted by İkinciKeleş[25] showed that a 900 MHz EMF applied in the prenatal period adversely affected the development of the vertebrae, and that this effect caused pathological changes in the vertebrae of rat pups. İkinciKeleş and BitergeSüt[5] reported that prenatal exposure to a 900 MHz EMF may produce adverse effects in the rat spinal cord, and that these may result in structural changes. Another study, by Eid et al. [26], reported that exposure to EMF caused neural damage in the hippocampus and cerebellum. Moussa et al. [27] also reported significant changes in the structure of the rat hippocampus exposed to EMF, especially in the CA3 region.

The main effect of EMF on biological systems occurs as a result of the production of free radicals [28]. The organism possesses various enzymatic and non-enzymatic antioxidant defence systems to cope with the effects of these harmful radicals. However, studies on the conditions that cause the balance between free radicals and antioxidants to deteriorate in favour of free radicals have shown that the use of antioxidant substances can minimize this oxidative stress by reducing neuronal damage through inhibition [29, 30]. The present study investigated the protective effects of antioxidant agents such as Mel and ω3 on neurodegeneration occurring in the spinal cord of rats exposed to 900 MHz EMF in the prenatal period by means of stereological and histopathological methods. Mel plays a

critically important role in foetal development and induces the proliferation of neural stem cells [31]. ErdemKoçet al. [32] used Mel to prevent the effects of EMF on the developing brain in the prenatal period and to protect the pyramidal neurons in the hippocampus region. Those authors observed that maternal Mel administration reduces the side-effects of EMF on the foetal brain. Delen et al. [33] showed that radiofrequency radiation (RFR) exposure caused structural deformation and apoptosis in brain tissue and that Mel ameliorated these deleterious effects of RFR. Another study conducted by Tüfekçi et al. [34] reported that Mel exhibited a neuroprotective effect on the optical nerve of rats exposed to prenatal EMF. One of the polyunsaturated fatty acids, ω3 plays an important role in the development of nervous system [35]. Bi et al. [36] showed that ω3 fatty acid supplementation reduced oxidative stress, apoptosis and levels of inflammatory markers in rats with spinal cord injury. Various studies have also reported positive effects of ω3 administration on neuronal morphology and numbers [32, 37, 38].

Stereological methods, which are used to obtain unbiased and effective results, make it possible to obtain three-dimensional quantitative information about objects by using their two-dimensional planar projections [39].In the present study, the physical disector, a stereological method, was used in calculating the numbers of spinal cord motor neurons in the groups.In addition, Cavalieri method was employed to estimate the volumes of the relevant structures [39, 40].In this study, the effects of prenatal EMF exposure on spinal cord motor neurons were evaluated and the possible neuroprotective roles of Mel and ω3 were investigated. Our findings revealed that the number of motor neurons decreased in the groups exposed to EMF in the prenatal period, and this decrease was significant especially in the EMF-ω3 group compared to both the control and the Mel group. This result suggests that ω3 alone may be insufficient to prevent the neurotoxic effects of prenatal EMF exposure. As is known, ω3 fatty acids are highly sensitive to oxidation. Therefore, ω3 may have triggered the oxidative effect originating from EMF during prenatal neurodevelopment. A combined application of ω3 with different antioxidants may be effective in treating the destructive effects originating from EMF. On the other hand, factors such as the bioavailability, duration of effect, and dosage of ω3 may also play a role in the treatment of EMF-induced damage. In addition to the EMF-induced changes in the number of motor neurons, no difference was observed between the groups in total spinal cord volume and volumetric fractions of gray and white matter. The damage occurring at the cellular level may not have been reflected by volumetric data. EMF damage triggers pathways related to oxidative stress and cell death mechanisms at the cellular level. Therefore, it is a more accurate approach to consider the

results at the neuronal level in the prenatal period.On the other hand, while neuron loss occurs in the prenatal period, volumetric changes may not have been observed due to glial proliferation. In this context, when evaluating the neurodevelopmental processes of EMF-induced damage in the central nervous system, the total number of oligodendrocytes and astrocytes should also be investigated to see real changes in the brain. In agreement with the criteria determined by Sugimoto et al. [20] for describing damaged neurons, the light microscopicresults of cresyl violet staining of the present study revealed that the cell boundaries of cells in EMF group were not clearly distinct and that neurons with a narrow and dark stained cytoplasm were more numerous compared with the CONT group. Oxidative stress caused by EMF exposure may induce apoptosis by leading to apoptotic signal production [41]. The presence of a large number of darkly stained cells in the spinal cord suggests apoptosis induced in cells following EMF exposure. In addition, in terms of ultrastructure, Meland ω3 administration minimized the neurodegenerative effects caused by EMF in the spinal cord. The histopathological protection provided by Mel, with its known strong neuroprotective effect, was higher than that caused by ω3. This can be attributed to Mel passing easily through physiological barriers due to its amphiphilic property. In addition, when the light microscopic results of semi-thin sections stained with toluidine blue were examined,it was seen that motor neurons and neuroglia cells had normal morphology in CONT, SHAM, Mel and ω3 groups.

When EMF, EMF-Mel and EMF-ω3 groups were examined, vacuolization around the neurons was noted. In this context, the electron microscopic results obtained in the present study also support these findings and reveal that Mel and ω3 minimize this effect in nerve damage caused by EMF. In addition, when the axonal structure was examined in all groups; it was observed that axons in CONT and ω3 groups exhibited a healthy morphology, while a small amount of axonal degeneration that did not affect the general morphology was seen in the SHAM group. In the Mel group, many axons with deteriorated morphology were detected. Apart from this, serious axonal degradation and oligodendrocyte degeneration were detected in the EMF group. In the EMF-Mel and EMF-ω3 groups, it was seen that the harmful effects of EMF were alleviated, and it was determined that there were plenty of healthy axons and oligodendrocytes that preserved their morphology. In this case, it can be said that Mel and ω3 may promote remyelination after toxic damage to central nervous system oligodendrocytes. Electro-hypersensitivity symptoms resulting from excessive exposure to telecommunication devices may occur due to damage to oligodendrocytes, which play an important role in myelin formation in the central nervous system [42].In the relevant study, the therapeutic effect of

Mel and ω3, especially on oligodendrocytes, in axonal damage caused by EMF is remarkable. In this context, the role of these neuroglia in nerve damage due to EMF exposure should be supported by further studies explaining detailed mechanisms.

CONCLUSION

This study has shown that ω3 treatment+exposure to 900 MHz EMF during the prenatal period creates toxic effect at the number of motor neuron in the spinal cord, but this side effect was not seen in terms of volume fraction. Our expectation in this experiment was to see toxic effects of EMF exposure on the motor neuron number and volume of spinal cord in the EMF group. Changes at the number of neuron level was observed only EMF-ω3 group. This may point that the developing nervous system is sensitive to a combined environmental stress factors such EMF and ω3. This discrepancy should be investigated. Further studies are needed to elucidate the mechanisms of a combined antioxidant with EMF exposure.

Conflicts of interest: Authors declare no conflicts of interest.
Funding: This research was supported by the Scientific and Technological Research Council of Türkiye (TÜBİTAK).
Submitted: May 4, 2025
Accepted: July 10, 2025
Published online: July 21, 2025

REFERENCES

[1] Samaila B, Sagagi YM, Tampul HM. Exposure and biological impacts assessment of non-ionizing electromagnetic radiation. Sci Set J Phys 2023;2:01-11.

[2] Ok F, Emre M, Bisgin A, Jafarguliyev S, Boga I, Cetiner S, et al. Effect of 900 MHz radiofrequency electromagnetic radiation emitted from mobile phone on testicular immunity and the associated risk of testicular germ cell tumor. TumorDiscov2024;3:1703. https://doi.org/10.36922/td.1703.

[3] İkıncı Keleş A, Erol HS, Sapmaz T, Mercantepe T, Keleş G, BıtergeSüt B, et al. Biochemical and pathological effects on the male rat hepatic tissue after exposure to 900mhz electromagnetic field during adolescent period. CommunFac Sci UnivAnk Ser C Biology 2021b;30:25-46. https://doi.org/10.53447/communc.764890.

[4] Sharma A, Shrivastava S, Shukla S. Oxidative damage in the liver and brain of the rats exposed to frequency-dependent radiofrequency electromagnetic exposure: biochemical and histopathological evidence. Free Radic Res 2021;55:535-46. https://doi.org/10.1080/10715762.2021.1966001.

[5] IkinciKeles A, BitergeSüt B. Histopathological and epigenetic alterations in the spinal cord due to prenatal electromagnetic field exposure: An H3K27me3-related mechanism. Toxicol Ind Health 2021a;37:189-97. https://doi.org/10.1177/0748233721996947.

[6] Deniz OG, Kaplan S. The effects of different herbals on the rat hippocampus exposed to electromagnetic field for one hour during the prenatal period. J Chem Neuroanat2022;119:102043. https://doi.org/10.1016/j.jchemneu.2021.102043.

[7] Diab YA, Alghannam MA, Gomaa RS, Abozaid ER. Effect of exposure to cell phone radiation on testicular function of male albino rats. ZagazigUniv Med J 2023;29:914-919. https://doi.org/10.21608/zumj.2021.78572.2248.

[8] Vafaei A, Raji AR, Maleki M, Zaeemi M, Ebrahimzadeh-bideskan A. Ameliorative effects of crocin against electromagnetic field-induced oxidative stress and liver and kidney injuries in mice. Avicenna J Phytomed2023;13:200-12. https://doi.org/10.22038/ajp.2022.21169.

[9] İkinci A, Mercantepe T, Unal D, Erol HS, Sahin A, Aslan A, et al. Morphological and antioxidant impairments in the spinal cord of male offspring rats following exposure to a

continuous 900 MHz electromagnetic field during early and mid-adolescence. J Chem Neuroanat2016;75:99-104. https://doi.org/10.1016/j.jchemneu.2015.11.006.

[10] Elamin AAE, Deniz OG, Kaplan S. The effects of Gum Arabic, curcumin (Curcuma longa) and Garcinia kola on the rat hippocampus after electromagnetic field exposure: a stereological and histological study. J Chem Neuroanat2022;120:102060. https://doi.org/10.1016/j.jchemneu.2021.102060.

[11] Galano A, Tan DX, Reiter RJ. Melatonin as a natural ally against oxidative stress: A physicochemical examination. J Pineal Res 2011;51:1-16. https://doi.org/10.1111/j.1600-079X.2011.00916.x.

[12] Tan HY, Ng KY, Koh RY, Chye SM. Pharmacological effects of melatonin as neuroprotectant in rodent model: a review on the current biological evidence. Cell Mol Neurobiol2020;40:25-51. https://doi.org/10.1007/s10571-019-00724-1.

[13] Sagrillo-Fagundes L, AssuncaoSalustiano EM, Yen PW, Soliman A, Vaillancourt C. Melatonin in pregnancy: effects on brain development and cns programming disorders. Curr Pharm Des 2016;22:978-86. https://doi.org/10.2174/1381612822666151214104624.

[14] Colella M, Biran V, Baud O. (2016). Melatonin and the newborn brain. Early Hum Dev 2016;102:1-3. https://doi.org/10.1016/j.earlhumdev.2016.09.001.

[15] Tucker I.M, Brown SD, Kanyeredzi A, McGrath L, Reavey P. Living 'in between' outside and inside: The forensic psychiatric unit as an impermanent assemblage. Health Place 2019;55:29-36. https://doi.org/10.1016/j.healthplace.2018.10.009.

[16] Shahidi F, Ambigaipalan P. Omega-3 polyunsaturated fatty acids and their health benefits. Annu Rev Food Sci Technol2018;9:345-81. https://doi.org/10.1146/annurev-food-111317-095850.

[17] Dighriri IM, Alsubaie AM, Hakami FM, Hamithi D, Alshekh MM, Khobrani FA, et al. Effects of omega-3 polyunsaturated fatty acids on brain functions: a systematic review. Cureus 2022;14:e30091. https://doi.org/10.7759/cureus.30091.

[18] Altunkaynak BZ, Önger ME, Altunkaynak ME, Ayrancı E, Canan S. A brief introduction to stereology and sampling strategies. NeuroQuantology2012;10:31-43. https://doi.org/10.14704/nq.2012.10.1.427.

[19] Denizci E, Altun G, Kaplan S. Morphological evidence for the potential protective effects of curcumin and Garcinia kola against diabetes in the rat hippocampus. Brain Res 2024;1839:149020. https://doi.org/10.1016/j.brainres.2024.149020.

[20] Sugimoto T, Bennett GJ, Kajander KC. Transynaptic degeneration in the superficial dorsal horn after sciatic nerve injury: effects of a chronic constriction injury, transaction and strychnine. Pain 1990;42:205-13.https://doi.org/10.1016/0304-3959(90)91164-E.

[21] Deniz OG, Kaplan S, Selcuk MB, Terzi M, Altun G, Yurt KK, et al. Effects of short and long term electromagnetic fields exposure on the human hippocampus. J MicroscUltrastruct2017;5:191-7. https://doi.org/10.1016/j.jmau.2017.07.001.

[22] Brent RL, Weitzman M. The vulnerability, sensitivity, and resiliency of the developing embryo, infant, child, and adolescent to the effects of environmental chemicals, drugs, and physical agents as compared to the adult: Preface. Pediatrics2004;113:933-4. https://doi.org/10.1542/peds.113.S3.932.

[23] Mohamed H, Deniz OG, Kaplan S. The neuroprotective effects of baobab and black seed on the rat hippocampus exposed to a 900-MHz electromagnetic field. J Chem Neuroanat2024;137:102405. https://doi.org/10.1016/j.jchemneu.2024.102405.

[24] Yahyazadeh A, Altunkaynak BZ. Effect of luteolin on biochemical, immunohistochemical, and morphometrical changes in rat spinal cord following exposure to a 900 mhz electromagnetic field. Biomed Environ Sci 2020;33:593-602. https://doi.org/10.3967/bes2020.078.

[25] İkinciKeleş A. Morphological changes in the vertebrae and central canal of rat pups born after exposure to the electromagnetic field of pregnant rats. Acta Histochem2020;122:151652. https://doi.org/10.1016/j.acthis.2020.151652.

[26] Eid AEZ, Salemb MF, Nosseira NS, El-Hanafy HAM. Effect of exposure to the electromagnetic waves emitted from cellular phone on the cerebellum and hippocampus of the adult male albino rats. Tanta Med J 2024;52:390-397. https://doi.org/10.4103/tmj.tmj_55_24.

[27] Moussa NAA, Farrag KAELR, Kalleny NK, Hamam GG. (2024). Effect of different methods of mobile phone exposure on the structure of hippocampus in adult albino rats. J MicroscUltrastruct 2024;272408477. doi: https://doi.org/10.4103/jmau.jmau_59_24.

[28] Terzi M, Ozberk B, Deniz OG, Kaplan S. The role of electromagnetic fields in neurological disorders. J Chem Neuroanat 2016;75(B):77-84. https://doi.org/10.1016/j.jchemneu.2016.04.003.

[29] Yıldırım M, Değirmenci U, Akkapulu M, Berköz M, Yalın AE, Çömelekoğlu Ü. The effect of rheum ribes L. extract on oxidative stress in heart tissue of diabetic rats. Van Health Sci J 2020;13:20-6. https://doi.org/10.1515/jbcpp-2020-0058.

[30] Olufunmilayo EO, Gerke-Duncan MB, Holsinger RMD. Oxidative stress and antioxidants in neurodegenerative disorders. Antioxidants 2023;12:517. https://doi.org/10.3390/antiox12020517.

[31] Li Z, Li X, Chan MTV, Wu WKK, Tan D, Shen J. Melatonin antagonizes interleukin-18-mediated inhibition on neural stem cell proliferation and differentiation. J Cell Mol Med 2017;21:2163-71. https://doi.org/10.1111/jcmm.13140.

[32] ErdemKoc G, Kaplan S, Altun G, Gumus H, Gulsum Deniz O, Aydin I, et al. Neuroprotective effects of melatonin and omega-3 on hippocampal cells prenatally exposed to 900 MHz electromagnetic fields. Int J RadiatBiol2016;92:590-5. https://doi.org/10.1080/09553002.2016.1206223.

[33] Delen K, Sırav B, Oruç S, Seymen CM, Kuzay D, Yeğin K, et al. Effects of 2600 MHz radiofrequency radiation in brain tissue of male wistar rats and neuroprotective effects of melatonin. Bioelectromagnetics2021;42:159-72. https://doi.org/10.1002/bem.22318.

[34] Tüfekci KK, Kaplan AA, Kaya AA, Alrafiah A, Altun A, Aktas A. The potential protective e!ects of melatonin and omega-3 on the male rat optic nerve exposed to 900 MHz electromagnetic radiation during the prenatal period. Int J Neurosci2023;133:1424-36. https://doi.org/10.1080/00207454.2023.2259078.

[35] Das UN. Biological significance of essential fatty acids. J Assoc Physicians India 2006;54:309-319.

[36] Bi J, Chen C, Sun P, Tan H, Feng F, Shen J. Neuroprotective effect of omega-3 fatty acids on spinal cordinjury induced rats. Brain and Behavior 2019;9:e01339. https://doi.org/10.1002/brb3.1339.

[37] Denis I, Potier B, Heberden C, Vancassel S. Omega-3 polyunsaturated fatty acids and brain aging. CurrOpin Clin NutrMetab Care 2015;18:139-46. https://doi.org/10.1016/j.arr.2013.01.007.

[38] Altun G, Kaplan S, Deniz OG, Kocacan SE, Canan S, Davis D, et al. Protective effects of melatonin and omega-3 on the hippocampus and the cerebellum of adult Wistar albino rats exposed to electromagnetic fields. J MicroscUltrastruct2017;5:230-41. https://doi.org/10.1016/j.jmau.2017.05.006.

[39] Yurt KK, Kıvrak EG, Altun G, Mohamed H, Ali F, Gasmalla HE et al. A brief update on physical and optical disector applications and sectioning staining methods in neuroscience. J Chem Neuroanat2018;93:16-29. https://doi.org/10.1016/j.jchemneu.2018.02.009.

[40] Candan M, Çakmak G. A morphological and stereological study on cervical spinal cord of one- and five-months age male rat. BEU J Sci Technol2020;9:143-56.

[41] Ozben T. Oxidative stress and apoptosis: impact on cancertherapy. J Pharm Sci 2007;96:2181-96. https://doi.org/10.1002/jps.20874.

[42] Johansson O, Redmayne M. Exacerbation of demyelinating syndrome after exposure to wireless modem with public hotspot. ElectromagnBiol Med 2016;35:393-7. https://doi.org/10.3109/15368378.2015.1107839.

TABLES AND FIGURES WITH LEGENDS

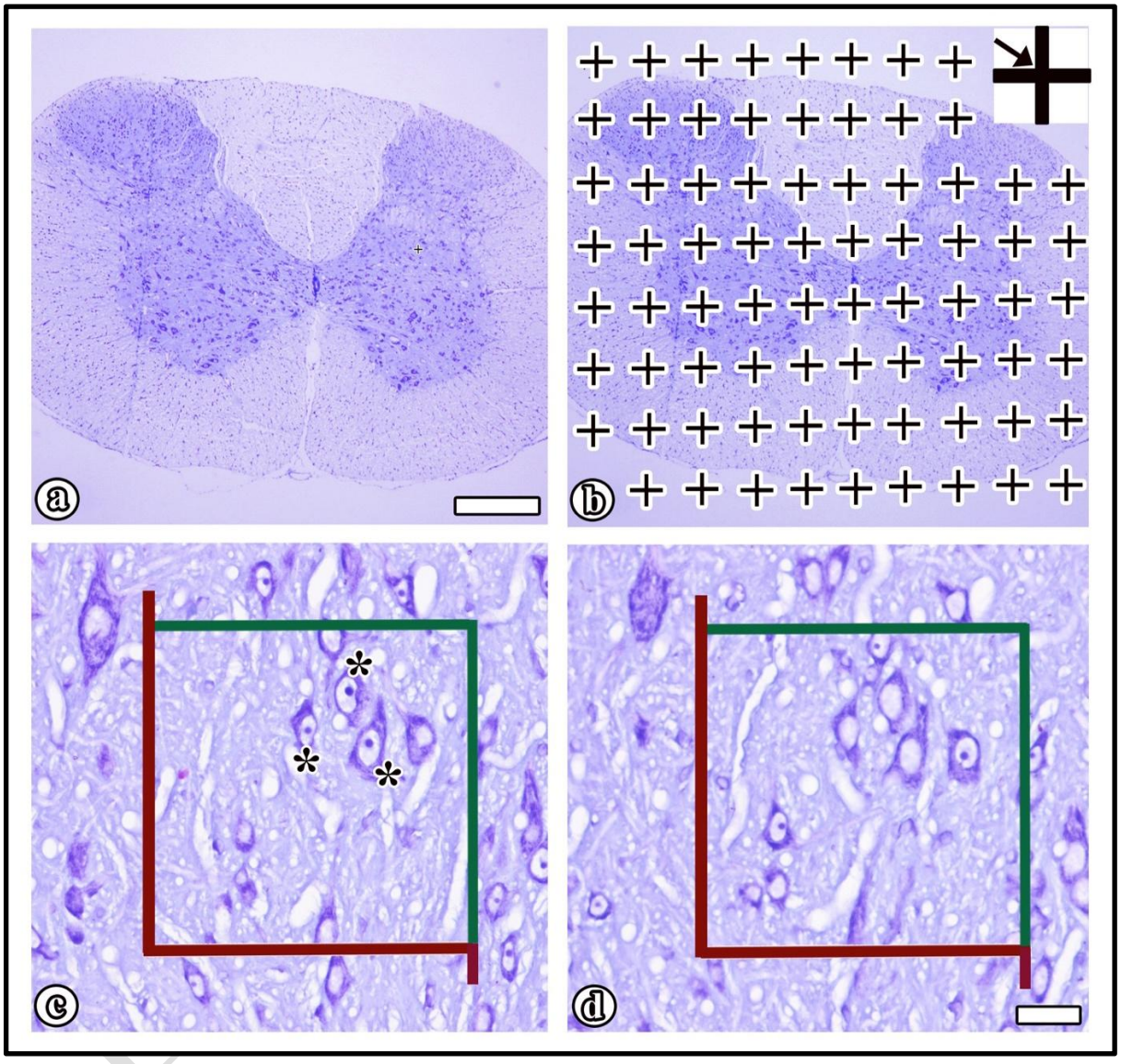

Figure 1. Representative micrographs showing the stereological application of the Cavalieri principle (a and b) and the physical dissector (c and d).

(a) Panoramic image of the spinal cord; (b) A dotted area ruler superimposed over the panoramic image to apply the Cavalieri principle; (c and d) Consecutive serial sections taken to apply the physical disector: (c) reference section; (d) look-up section. Red lines within the counting frame show the forbidden edges, while green lines show the included edges. (*): These indicate the disector particles, nucleoli that are seen in reference section but not in look

up section, can be counted according to the counting frame and the physical disector rules. Original magnification: ×100.

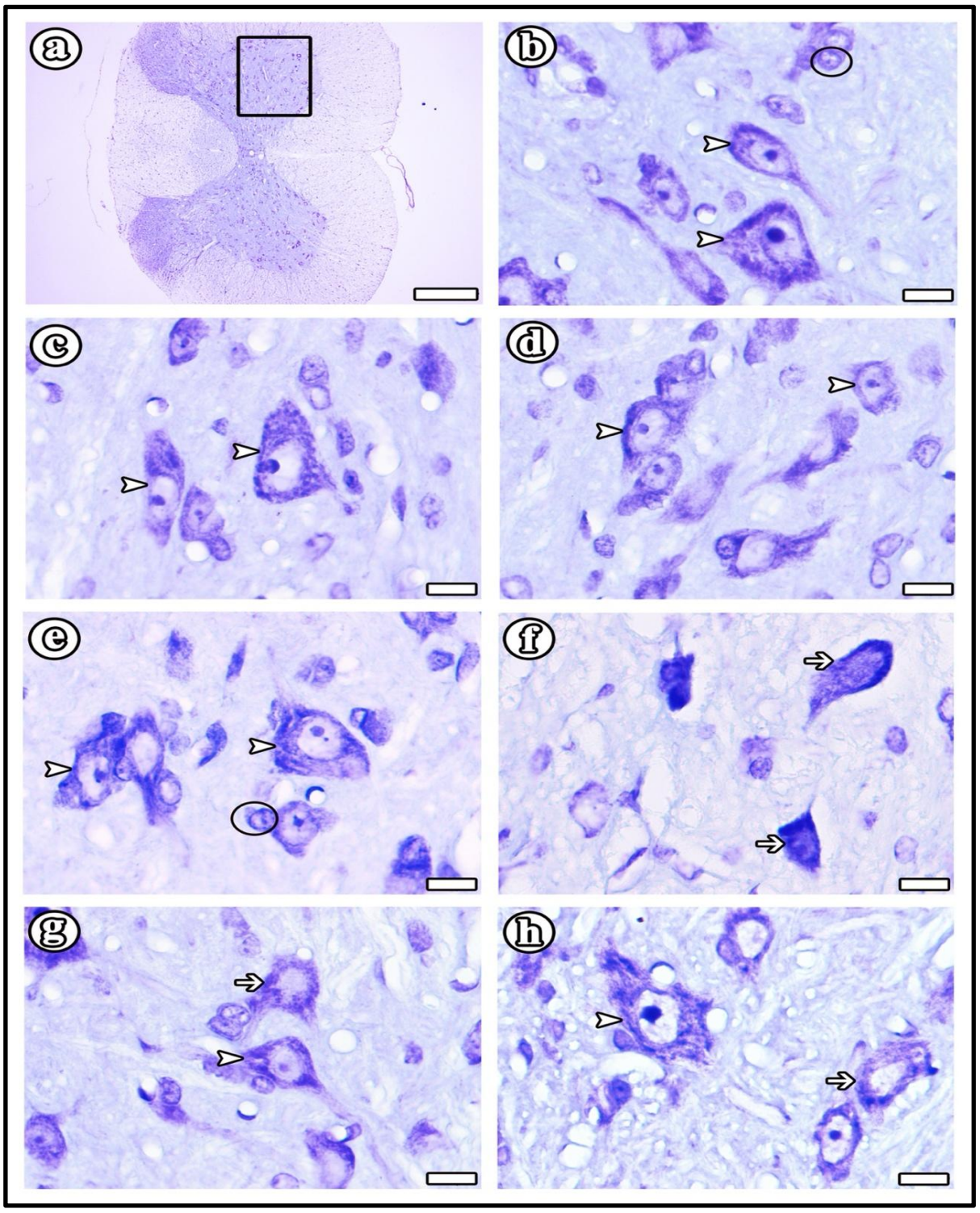

Figure 2. (a-h) Cresyl violet-stained spinal cord sections after 2-hour exposure to EMF.

(a) Panoramic view of the spinal cord; (b) CONT group; (c) SHAM group; (d) Mel group; (e) ω3 group; (f) EMF group; (g) EMF-Mel group; (h) EMF-ω3 group. Arrowhead: Healthy motor neurons; Arrow: Degenerated motor neurons; Circle: Glia cell. Original magnification: ×100.

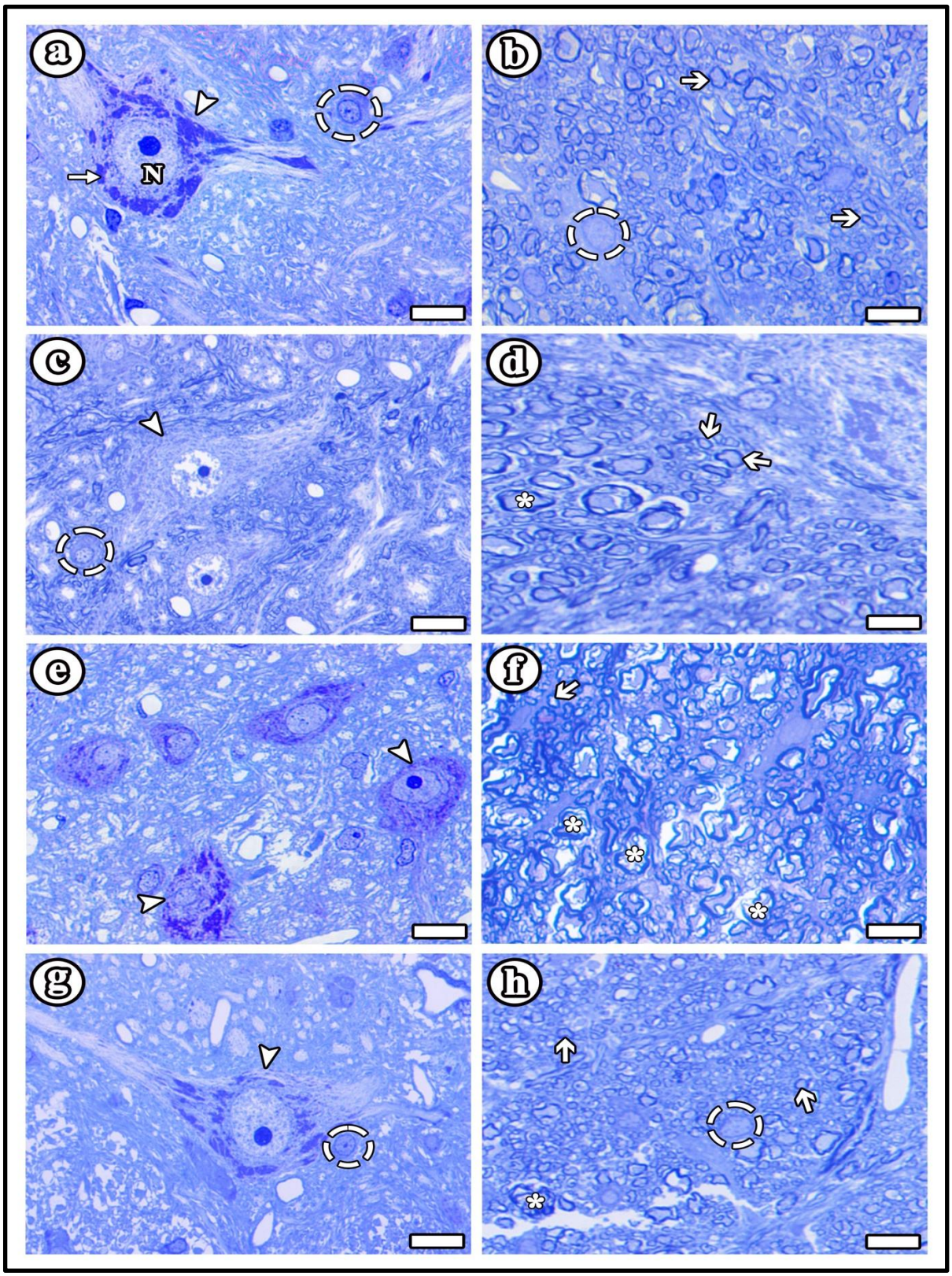

Figure 3. (a-h) Light microscope images of the groups are presented in semi-thin sections. (a, b) CONT group; (c, d) SHAM group; (e, f) Mel group; (g, h) ω3 group. Arrowhead: Healthy motor neuron; Thin arrow: Nissl body; Thick arrow: Healthy myelinated axon structure; Dashed circle: Healthy oligodendrocyte; (*): Degenerated myelinated axon; N: Nucleus. Scale bars: 10 μm-toluidine blue staining.

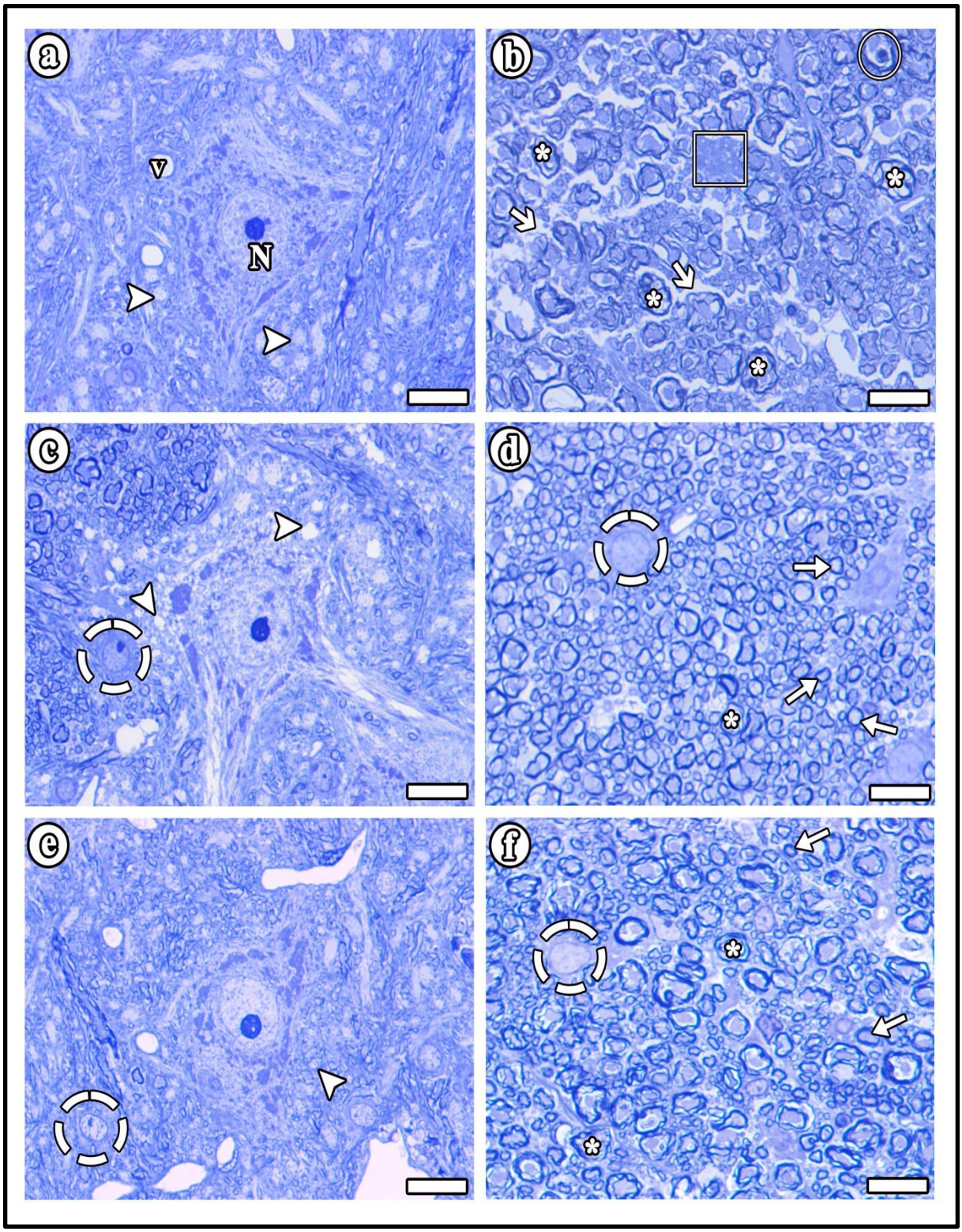

Figure 4. (a-f) Light microscope images of the groups are presented in semi-thin sections. (a, b) EMF group; (c, d) EMF-Mel group; (e, f) EMF-ω3 group. Arrowhead: Vacuolization around motor neurons; Thin arrow: Healthy myelinated axon structure; Thick arrow: Endoneurial disruption; Dashed circle: Healthy oligodendrocyte, (*): Degenerated myelinated

axon; Circle: Schmidt-Lanterman cleft; Rectangle: Degenerated oligodendrocyte; N: Nucleus; v: Vessel. Scale bars: 10 µm-toluidine blue staining.

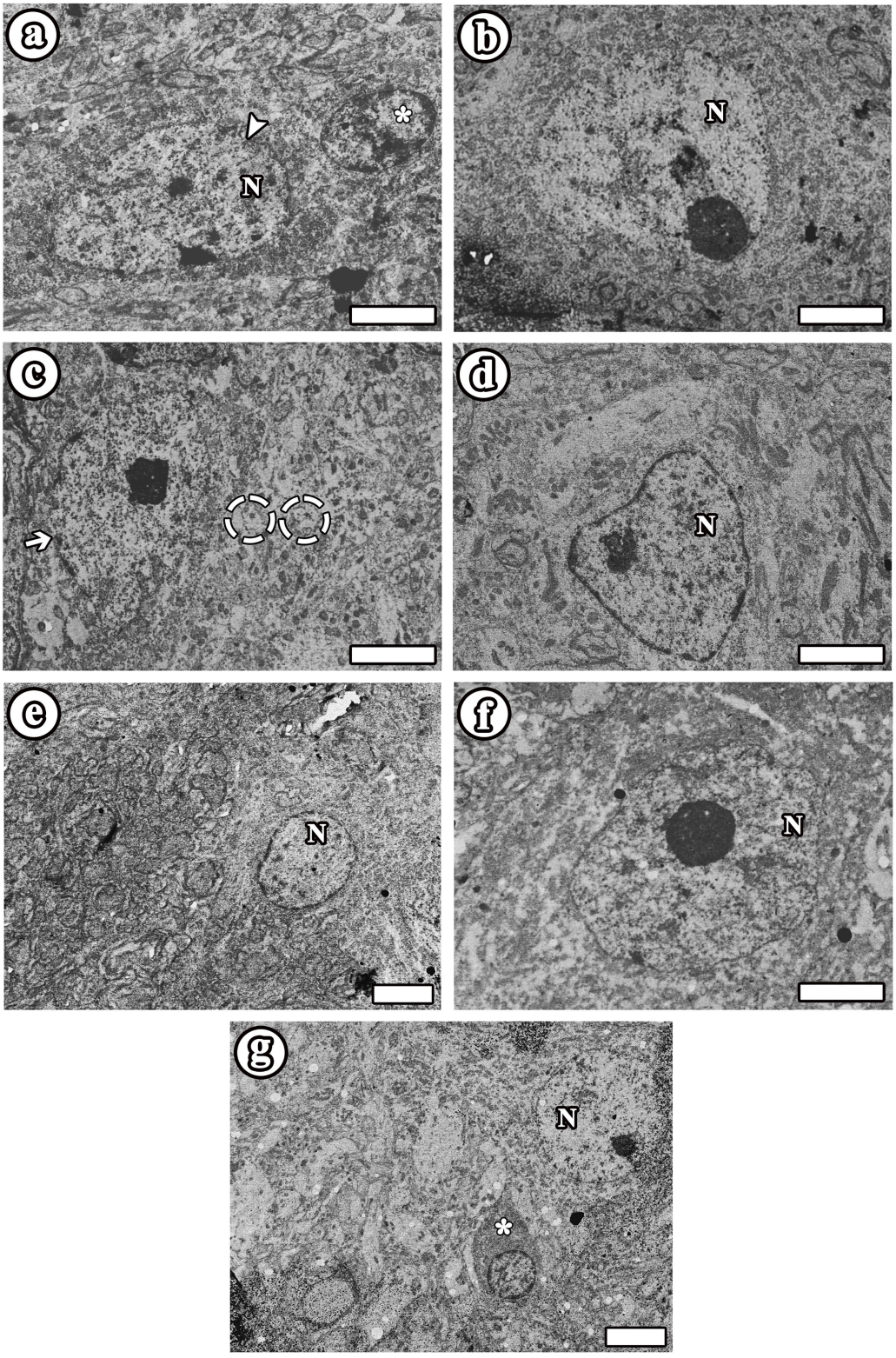

Figure 5. (a-g) Electron microscope images of the groups are seen taken from thin sections. **(a)** CONT group; (b) SHAM group; (c) EMF group; (d) EMF-Mel group; (e) EMF-ω3 group; (f) Mel group; (g) ω3 group. Arrowhead: Healthy motor neuron; Arrow: Neuron with disrupted membrane integrity; Dashed circle: Vacuolization around motor neuron; (*): Healthy oligodendrocyte; N: Nucleus. Scale bars: 1 μm.

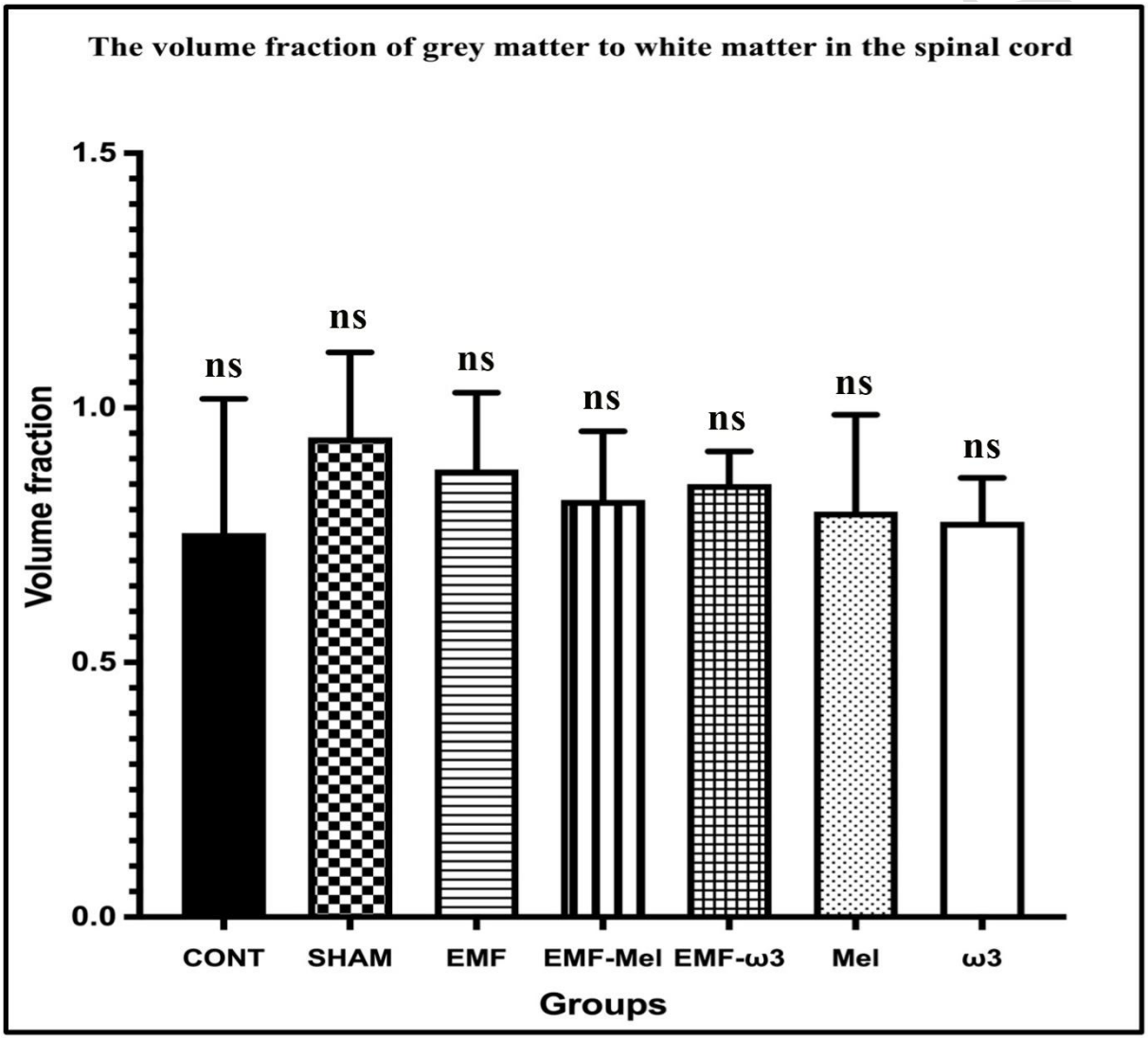

Figure 6. Graph illustrating group differences in spinal cord GM/WM volume following 2-hour EMF exposure. No statistically significant differences were observed between the groups ($p > 0.05$); non-significance is indicated by ns.

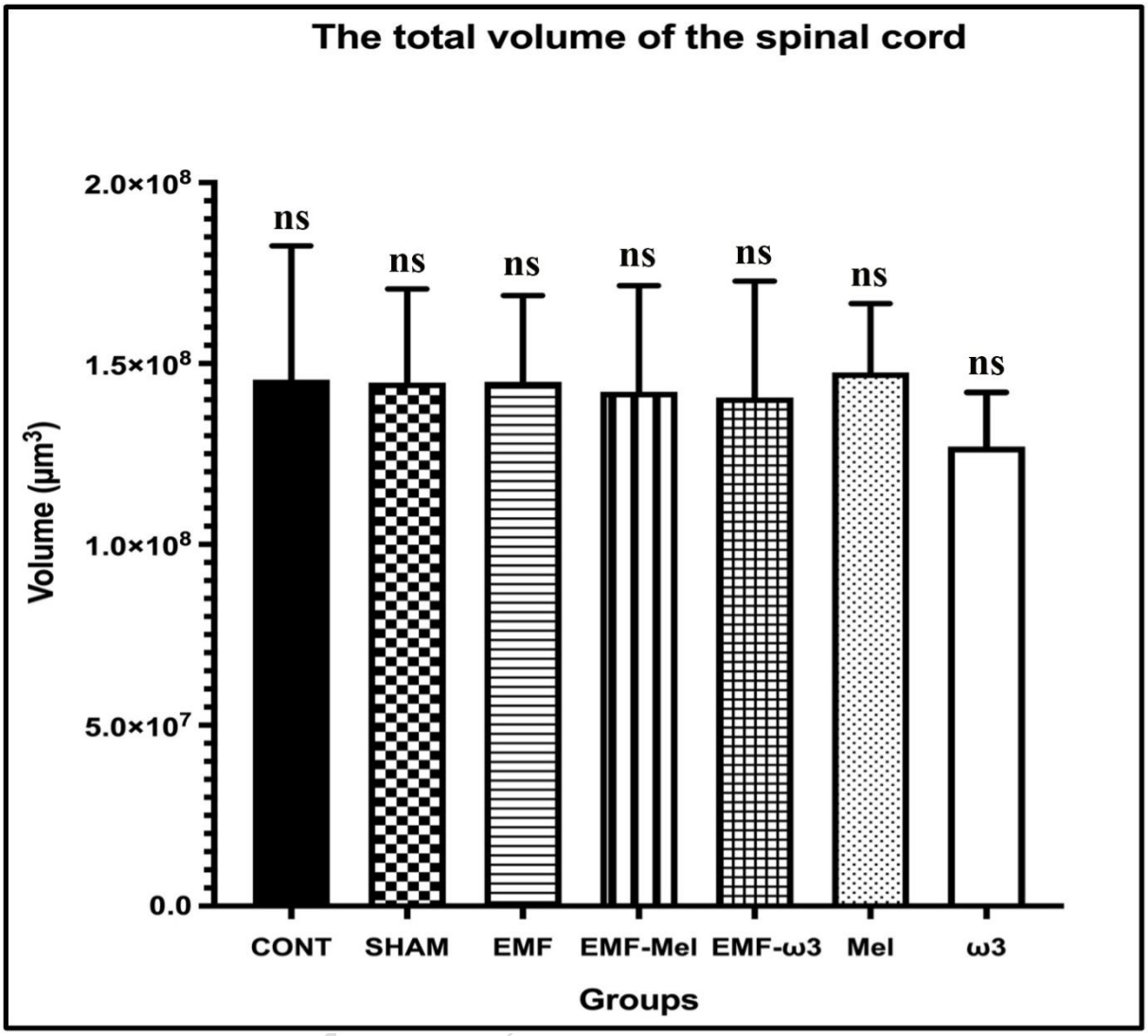

Figure 7. Graph illustrating group differences in total spinal cord volume following 2-hour EMF exposure. No statistically significant differences were observed between the groups ($p > 0.05$); non-significance is indicated by ns.

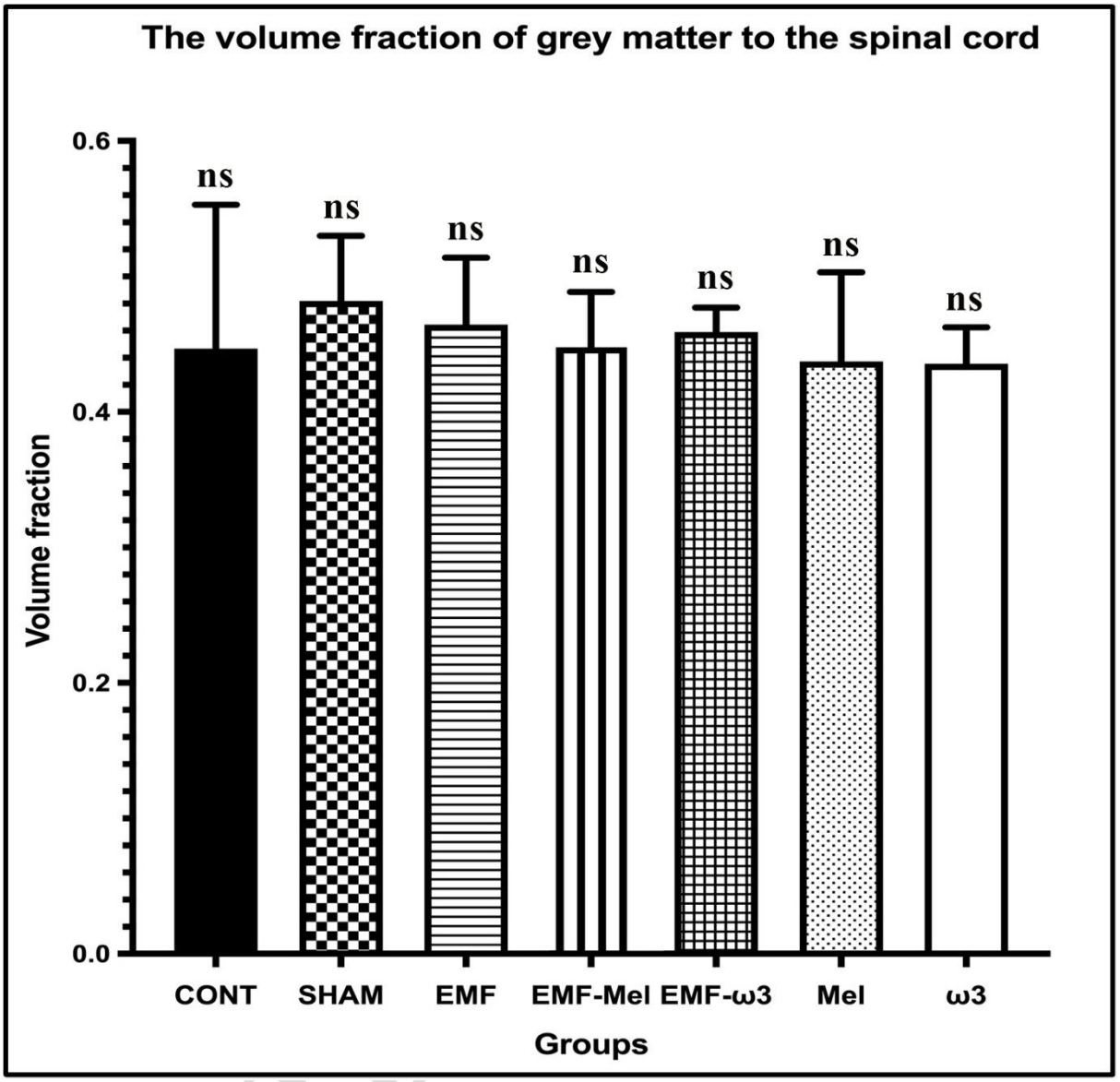

Figure 8. Graph illustrating group differences in GM/total volume ratio following 2-hour EMF exposure. No statistically significant differences were observed between the groups ($p > 0.05$); non-significance is indicated by ns.

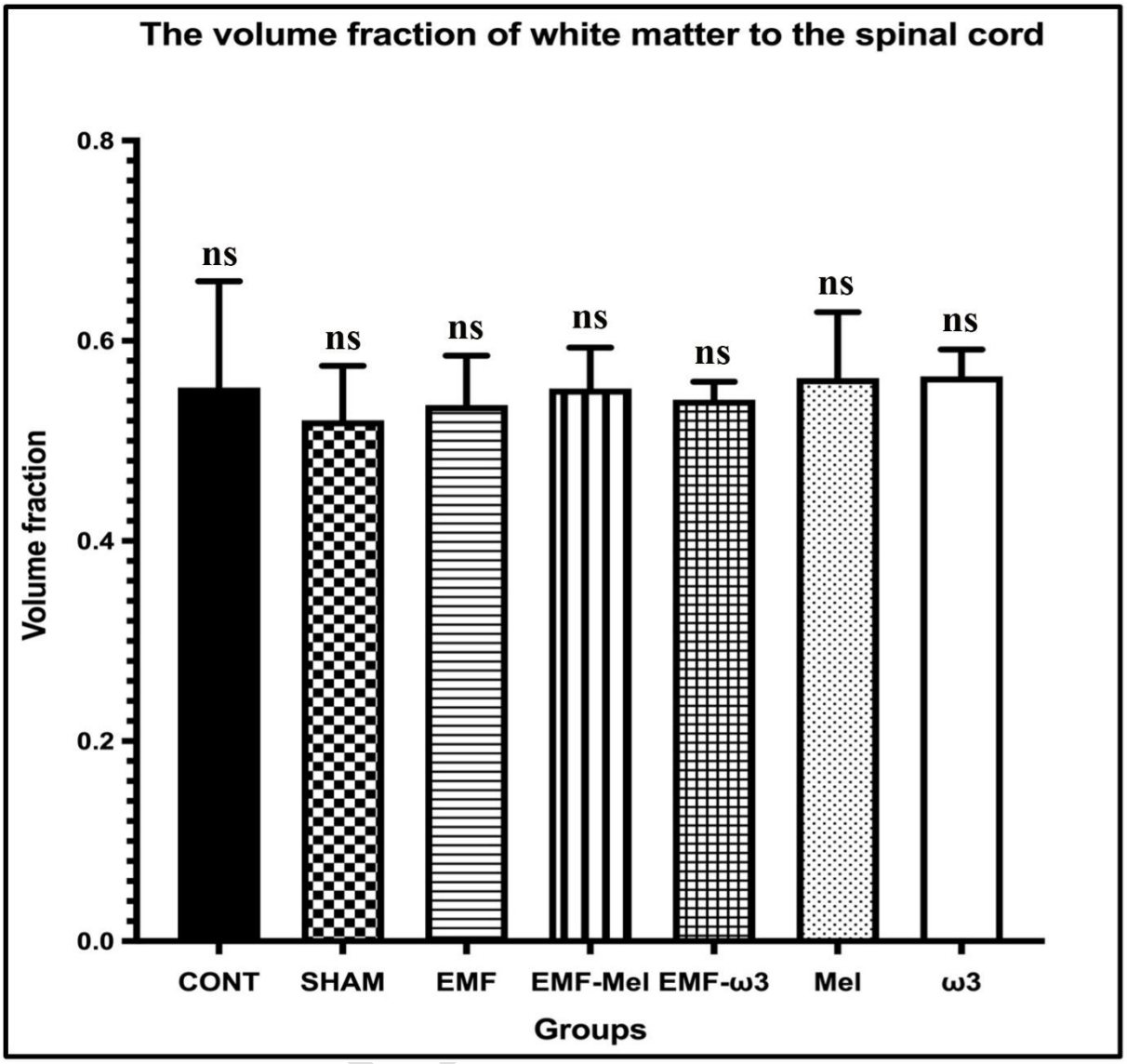

Figure 9. Graph illustrating group differences in WM/total volume ratio following 2-hour EMF exposure. No statistically significant differences were observed between the groups ($p > 0.05$); non-significance is indicated by ns.

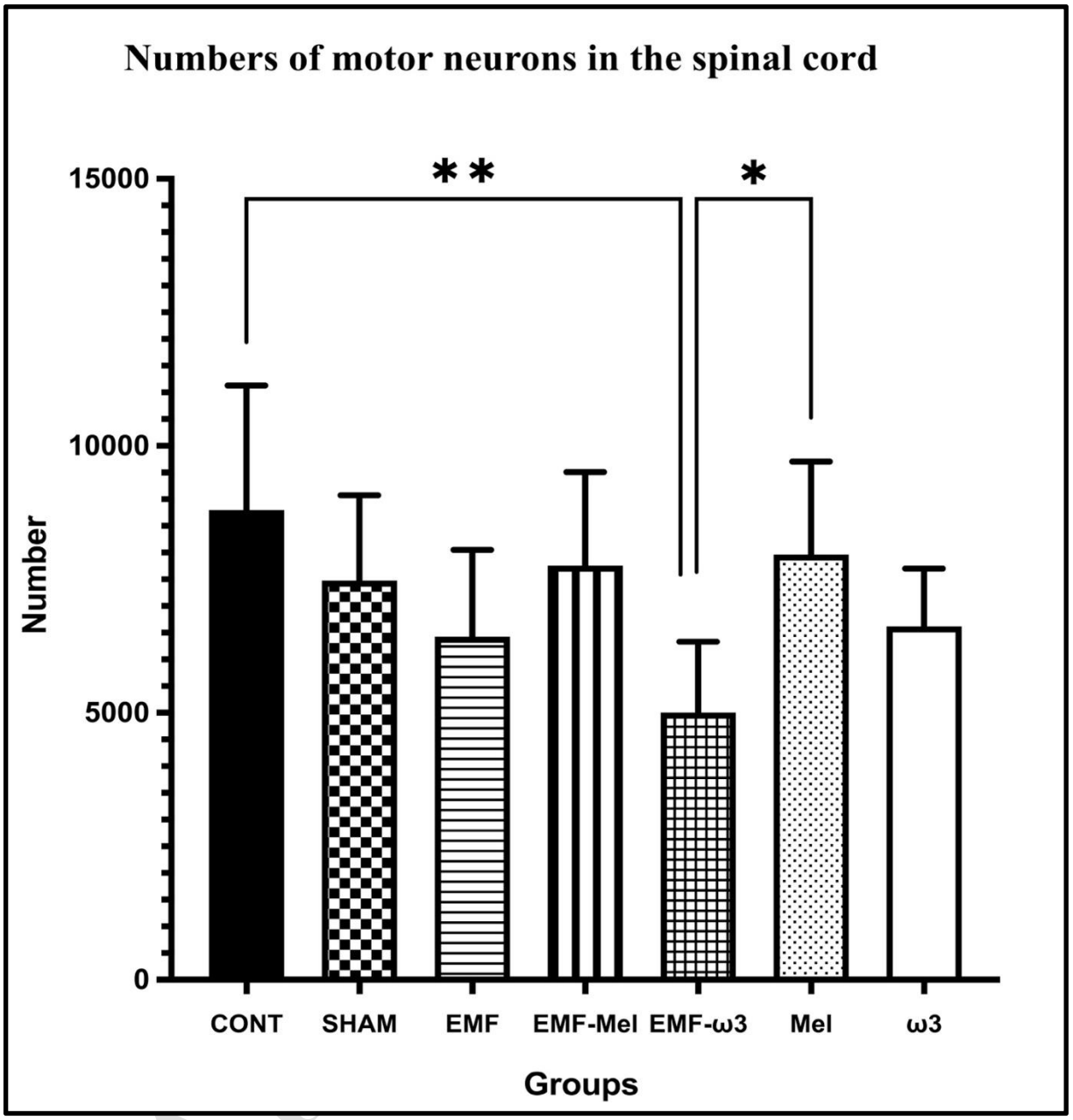

Figure 10. Graph illustrating group differences in the number of motor neurons in the spinal cord following 2-hour EMF exposure. Statistically significant differences are indicated as follows: $p < 0.05$ (*), $p < 0.01$ (**).